Molecular subgrouping of Atypical Teratoid / Rhabdoid Tumors (ATRT) – a reinvestigation and current consensus

Ben Ho[1,*], Pascal D. Johann[2,3,4*], Yura Grabovska[5,*], Mamy Jean De Dieu Andrianteranagna[6,7], Fu Pan Yao[8], Michael Frühwald[9], Martin Hasselblatt[10], Franck Bourdeaut[6,7], Daniel Williamson[5,#], Annie Huang[1,#,*], Marcel Kool[2,3, #,*]

1. Division of Hematology & Oncology, Arthur and Sonia Labatt Brain Tumour Research Centre, The Hospital for Sick Children, Toronto, ON, Canada. (BH, AH)
2. Hopp Children's Cancer Center (KiTZ), 69120 Heidelberg, Germany. (PDJ, MK)
3. Division of Pediatric Neurooncology, German Cancer Research Center (DKFZ) and German Cancer Research Consortium (DKTK), 69120 Heidelberg, Germany. (PDJ, MK)
4. Department of Pediatric Hematology and Oncology, University Hospital Heidelberg, 69120 Heidelberg, Germany. (PDJ)
5. Wolfson Childhood Cancer Research Centre, Northern Institute for Cancer Research, Newcastle University, Newcastle upon Tyne, UK. (YG, DW)
6. Departments of Genetics and of Oncopediatry and Young Adults, Curie Institute, Paris, France. (MJDDA, FB)
7. INSERM U830, Laboratory of Translational Research in Pediatric Oncology, SIREDO Pediatric Oncology Center, Curie Institute, Paris, France. (MJDDA, FB)
8. Department of Medical Biophysics, Faculty of Medicine, University of Toronto, Toronto, Canada. (FPY)
9. University Children's Hospital Augsburg, Swabian Children's Cancer Center, 86156 Augsburg, Germany. (MF)
10. Institute of Neuropathology, University Hospital Münster, 48149 Münster, Germany. (MH)

* Shared first authors

Shared senior authors

* Corresponding authors

Corresponding authors:

1. Marcel Kool, PhD

   Hopp Children's Cancer Center (KiTZ)

   Im Neuenheimer Feld 280

   69120 Heidelberg

   Germany

   Tel: +49-6221-424636

   Fax: +49-6221-424639

   Email: m.kool@kitz-heidelberg.de

2. Annie Huang, MD PhD

   The Hospital for Sick Children

   Division of Hematology & Oncology

   555 University Ave

   Toronto, Ontario

   Canada M5G 1X8

   Email: annie.huang@sickkids.ca

Funding

BH, FPY and AH are supported by Canadian Cancer Society Research Institute (CCSRI) (705056), the Canadian Institutes of Health Research (CIHR) project grant (409302) and Tali's fund. PDJ and MH are supported by the Deutsche Forschungsgemeinschaft (DFG) (JO 1598/1-1 and HA 3060/8-1, respectively). YG and DW are supported by grants from the INSTINCT network, The Brain Tumor Charity, Great Ormond Street Children's Charity, Children with Cancer UK (16/193), CRUK center core and Love Oliver. FB is supported by 101 des Arts, Abigael, Marabout de Ficelle, Etoile de Martin, Enfants et Cancer, St. Baldrick Robert Arceci Innovation award and the French Society for the Fight against Cancer and Leukemia in Children and Adolescents (SFCE).

Conflict of Interest

The authors declare no conflicts of interest.

Authorship

BH, PDJ, YG, FPY, and MDDJA, performed data analyses and generated all figures. MF, MH, FB, DW, AH, and MK contributed to data, concept and design of the paper. DW, AH and MK supervised data analyses. All authors contributed to the writing of the paper.

Abstract

Background: Atypical Teratoid / Rhabdoid Tumors (ATRT) are known to exhibit molecular and clinical heterogeneity even though *SMARCB1* inactivation is the sole recurrent genetic event present in nearly all cases. Indeed, recent studies demonstrated three molecular subgroups of ATRTs that are genetically, epigenetically and clinically distinct. As these studies included different numbers of tumors, various subgrouping techniques and naming, an international working group sought to align previous findings and to reach a consensus on nomenclature and clinic-pathologic significance of ATRT subgroups.

Methods: We integrated various methods to perform a meta-analysis on published and unpublished DNA methylation and gene expression datasets of ATRTs and associated clinico-pathological data.

Results: In concordance with previous studies, the analyses identified three main molecular subgroups of ATRTs, for which a consensus was reached to name them ATRT-TYR, ATRT-SHH, and ATRT-MYC. The ATRT-SHH subgroup exhibited further heterogeneity segregating further into two subtypes associated with a predominant supratentorial (ATRT-SHH-1) or infratentorial location (ATRT-SHH-2). For each ATRT subgroup we provide an overview on its main molecular and clinical characteristics, including *SMARCB1* alterations and pathway activation.

Conclusions: The introduction of a common classification, characterization and nomenclature of ATRT subgroups will facilitate future research and serve as a common ground for subgrouping patient samples and ATRT models, which will aid in refining subgroup-based therapies for ATRT patients.

Keywords:

ATRT, molecular subgroups, meta-analysis, consensus

Importance of the study

The international consensus on number and naming of ATRT molecular subgroups and their main characteristics, which we present here, will be important for the design of future clinical trials, patient stratification and a uniform classification of patient's tumor samples, much in line as it has been for medulloblastoma, ependymoma and high grade glioma. It will also be essential for a better interpretation of preclinical experiments using properly classified *in vitro* and *in vivo* ATRT models.

Introduction

Atypical Teratoid / Rhabdoid Tumors (ATRT) arise in all compartments of the central nervous system (CNS), predominantly affect infants or young children, and display a remarkably simple cancer genome. Bi-allelic mutation, including partial or whole loss of chromosome 22, resulting in inactivation of *SMARCB1* are the main - and often only - recurrent molecular features seen in ATRT[1]. Rare cases (<5%) with an intact *SMARCB1* harbor mutations in *SMARCA4*, both encoding components of the SWI/SNF chromatin remodeling complex[2,3]. The recurrent loss of SMARCB1 in these tumors is in stark contrast to a pleomorphic histology and considerable molecular and clinical heterogeneity observed in ATRT cohorts. Therapeutic strategies in ATRT are largely influenced by the age of the patient, tumor location in the CNS and disease stage at diagnosis[4]. These factors inform extent of surgical resection and various radiological and chemotherapeutic interventions. However, there is currently no international consensus on standard therapeutic approaches with the majority of therapeutic and survival data being published on a center-by-center basis. Numbers of patients with ATRT are small, therefore concerted international efforts to evaluate and standardize therapy are ongoing. However, it is as yet unclear how tumor biology shapes the response to treatment, outcome and/or long-term effects in patients with ATRT. A critical step towards improving the poor

outlook for these patients is therefore to define and characterize the biological heterogeneity in ATRT such that a standard subgrouping scheme is available and can be further used to investigate subgroup specific features of ATRT and inform subgroup specific therapies.

Earlier attempts to subgroup ATRT at the transcriptomic level had already recognized a degree of heterogeneity, but were limited by a small cohort size[5]. More recently, international efforts to collect and profile significantly larger cohorts of ATRTs have resulted in the identification of distinct ATRT subgroups defined by gene expression and/or DNA methylation profiling and associated with different molecular and clinico-pathological features (Table 1)[6-8]. Since the number of subgroups and platforms used to identify these subgroups differed between studies, there is an urgent need to align findings and define the number, molecular and clinical features and a common nomenclature for ATRT subgroups.

To this end, we performed a meta-analysis of previously published and additional ATRT DNA methylation profiles with parallel transcriptomic and clinico-pathological data in order to generate a consensus definition and naming for ATRT subgroups and to define their main molecular and clinico-pathological characteristics.

Materials and Methods

Integrated analyses of ATRT profiling data

Due to the variety of datatypes and platforms used previously to subgroup ATRT, we first created a composite data set of all cases (n = 388), profiled using the Illumina Infinium HumanMethylation 450K or EPIC arrays. We excluded all samples (n = 5), which were either duplicates or relapse cases. To exclude cases with a low tumor content or outliers for which a high-confidence classification of ATRT could not be achieved, we removed all samples (n = 58) with a calibrated score < 0.9 using the Heidelberg brain tumor classifier published in Capper *et al.*[9] (www.molecularneuropathology.org).

This filtering step aimed to identify potential outlier samples, and generated a high-quality reference dataset for classification of subgroups. A number of factors could contribute to a sample failing to be classified as ATRT with high-confidence including high non-neoplastic cell content and low quality tumor material from archival samples.

Of remaining 325 samples, 137 had been published in Johann *et al.*[8], 2016, 96 in Torchia *et al.*, 2016[7], and 92 are newly added unpublished samples from the Northern Institute of Cancer Research (Newcastle University) (GEO accession no. GSE141363) and the EURHAB study (GEO accession no. GSE141039) (Supplementary Table 1). Informed consent was obtained for all cases. In order to determine consensus subgroups, methylation array data were subjected to three different clustering methods, including consensus non-negative matrix factorization (NMF) (Schwalbe *et al.*, 2017[10]), regular NMF (Torchia *et al.*, 2015 & Torchia *et al.*, 2016[6,7]) and unsupervised consensus clustering (Johann *et al.*, 2016[8]) (Supplementary Methods for full technical details). Algorithms chosen had either been previously applied to discover ATRT subgroups or used in consensus subgrouping studies for other CNS tumors (i.e. Medulloblastoma[11]).

Consensus calls were established by comparison of calls from the three different methods, and consensus subgrouping was based on at least equivalent calls from two of the three methods. A "no consensus call" was assigned in four cases. As an additional validation step, we corroborated consensus calls using *t*-distributed stochastic neighbor embedding (*t*-SNE) analysis of the consensus dataset.

To corroborate DNA methylation based classification, we also reanalyzed published Affymetrix HG-U133 Plus2.0 expression profiles (n = 97)[8,12] and Illumina HT12 v4 gene expression array data (n = 60)[6] (Supplementary Methods for further information).

Results

DNA methylation and gene expression profiling identify three main subgroups of ATRT

Robust DNA methylation data from 325 unique ATRT cases (Fig. 1) were classified using three independent clustering algorithms (consensus NMF, regular NMF, ConsensusClusterPlus) to define consensus subgroups of ATRTs. Each method was applied considering a number of possible subgroups between two and eight. Clustering metrics (including but not limited to cophenetic coefficients, change in area under the cumulative distribution function (CDF) curve, dispersion, Kappa, Silhouette score, Supplementary Fig.1) indicated that the most consistently robust clustering solution was three subgroups with possible further subclusters identified, as previously discussed in Johann *et al.*[8], but supported less robustly here (Fig. 2, Supplementary Fig. 1). There was very high concordance between subgrouping based on consensus clustering (97%, 316 cases correctly classified), NMF (98%, 318 cases correctly classified), and consensus NMF (99%, 321 cases correctly classified), as shown in the Sankey plot in Fig. 2C. Notably, adding back samples excluded for low classification calls did not alter number of subgroups as indicated in the *t*-SNE analysis and cluster metrics for the methylation array analyses (Supplementary Fig. 2).

Given that each clustering method consistently identified three main subgroups of ATRTs, with a high degree (>90%) of concordance between the different methods applied (Fig. 2), we chose this as the basis of our consensus subgrouping. As shown in Fig. 2A-B, Group 1 annotated cases from the Torchia *et al*. study[7] formed one group with the ATRT-SHH cases from the Johann *et al*. study[8], while Group 2A and Group 2B annotated cases form groups with either ATRT-TYR or ATRT-MYC cases, respectively, indicating that our previous studies identified largely the same three subgroups.

We have designated the three subgroups as ATRT-SHH, ATRT-TYR and ATRT-MYC, based on the nomenclature proposed by Johann *et al.*[8].

We next analyzed ATRT gene expression profiles available for a total of 172 cases, profiled on Affymetrix HG-U133 Plus2.0 arrays (112, including 15 new cases) or Illumina HT-12 v4 arrays (60 cases)[6]. For 21 Affymetrix cases and for 48 Illumina profiled tumors there was matching DNA methylation data. Unsupervised hierarchical clustering analysis of the Affymetrix data using expression of the 1500 most variable genes confirmed the presence of three major molecular subgroups of ATRTs in line with DNA methylation analyses (Fig. 3A). These results remained stable across different numbers of differentially expressed genes (data not shown). Subgroup annotations were also highly concordant with prior publications where subsets of these data have been analyzed[8,12]; annotated hIC1 cases largely overlapped with the ATRT-SHH cases (8/10), while hIC2 and hIC3 annotated cases largely overlapped with ATRT-TYR cases (10/12) or ATRT-MYC cases (5/5), respectively (Fig. 3A). For the 21 cases with matched Affymetrix gene expression and DNA methylation data there was also good concordance with only two samples annotated to different subgroups. We assigned final annotation of these two cases based on the DNA methylation data. Similarly, unsupervised hierarchical clustering of the Illumina gene expression data also revealed three molecular subgroups of ATRTs with a good concordance (96%) between DNA methylation array and Illumina based subgrouping (Supplementary Fig. 3). It is worth noting that the clustering metrics derived from the Affymetrix data also supported three main and not additional subgroups (Supplementary Fig. 4B).

Finally, in order to gain further insights into the biology of the subgroups, we performed ingenuity pathway and gene set enrichment analyses for which the normalized enrichment scores are shown in Fig. 3B as a radar plot. Overall, the ATRT-SHH subgroup displayed a low overlap of enriched gene sets with ATRT-TYR and ATRT-MYC, but there was some overlap between ATRT-TYR and ATRT-MYC – in particular for gene sets related to immune response. The specific gene

enrichment features as well as comments on known published genes for each subgroup separate are described below.

Molecular and clinical features of the three subgroups

Having identified and confirmed the presence of three main molecular subgroups of ATRTs, we examined available pooled molecular and clinico-pathological data of all cases to define the main characteristics of each group as described below and shown in Fig. 4 (and an overview on cytogenetic aberrations in Supplementary Fig. 5).

Correlations of the three subgroups with published ATRT models.

In the last years, a number of cell lines and genetically engineered mouse models have been established to model ATRT tumorigenesis. In order to see how these match our consensus human ATRT subgrouping, we collected RNAseq and gene expression data from previously published studies[12-14] and performed a Multidimensional scaling (MDS) analysis, sample-wise correlation between cell lines and mouse models against human ATRT samples (Supplementary Fig. 6A,C), and unsupervised hierarchical clustering analysis on the combined human and mouse datasets using orthologous genes (Supplementary Fig. 6B). Results of this preclinical model characterization are discussed below in the respective sections.

ATRT-TYR

The ATRT-TYR subgroup was named after the enzyme tyrosinase, which is highly overexpressed in most ATRT-TYR cases, but not in the other ATRT subgroups or other brain tumors, indicating it may be a good diagnostic marker for ATRT-TYR cases[15]. The protein physiologically catalyzes the synthesis

of melanin in melanocytes and is an important protagonist in neural tube development[16]. Although the role of TYR in ATRT tumorigenesis remains to be established, it is notable that several other components of the melanosomal pathway, including the tyrosinase related protein *TYRP* and the melanoma-oncogene *MITF*, are also upregulated in this subgroup, potentially reflecting restricted neuroectodermal origins[17].

Other pathways and genes upregulated in ATRT-TYR tumors include the BMP-pathway (e.g. *BMP4*) and developmentally related transcription factors such as *OTX2* (Supplementary Fig. 4A). Gene set enrichment analysis performed on the differentially overexpressed genes confirms the melanosomal pathway and tyrosine metabolism (Fig. 3B, "GO [developmental] Pigmentation", "GO Pigment granule organization") as well as epithelial proliferation as being enriched in ATRT-TYR (Fig. 3B). Although comprehensive histopathological studies of ATRT molecular subtypes remain pending, it is notable that cribriform neuroectodermal tumors (CRINET), which also all express *TYR*, have DNA methylation profiles that are highly similar to ATRT-TYR tumors[18], suggesting that CRINET and ATRT-TYR tumors may represent two histological variants with a common cell of origin. Whether the favorable outcomes of CRINET patients[18] also applies to patients with ATRT-TYR tumors remains to be investigated.

Genetically, the prototypic type of bi-allelic *SMARCB1* inactivation in the ATRT-TYR group is whole or partial loss of one copy of chromosome 22 accompanied by an inactivating (e.g. point-) mutation in *SMARCB1* on the other allele (Fig. 4C-D). The loss of chromosome 22 was more prevalent in ATRT-TYR (86 versus 59 cases in ATRT-SHH and 16 cases in ATRT-MYC; $p = 0.053$, chi square test). Investigations using ATAC-seq revealed that this subgroup harbors a more open chromatin, suggestive of a more primitive epigenetic landscape as compared to the other ATRT subgroups[7].

Clinically, ATRT-TYR patients represent the youngest patient group with median age at diagnosis of 12 months (range 0 – 108 months). This subgroup also contained the highest proportion

of patients under three years at time of diagnosis (90% in ATRT-TYR vs 74.6% in ATRT-SHH vs 52.3% in ATRT-MYC (Fig. 4A, Supplemental Table 1). Most (75%, 52 of 69 with location data) ATRT-TYR tumors have infratentorial location and only 25% (17 cases) are located supratentorially (Fig. 4B). This differs significantly from ATRT-SHH and ATRT-MYC, which are more often localized supratentorially (p-value = 2.21e-09, chi square test). A recent radiogenomics study of ATRT molecular subgroups suggested that ATRT-TYR tumors may have MRI appearance characterized by a band like enhancement of contrast media[19].

For preclinical studies, the number of available *in vitro* and *in vivo* models for ATRT remains very limited and the number of models with molecular subgroup information is even more limited. In a recently published study by Brabetz *et al*.[20], three ATRT patient xenograft models from the SHH and MYC subgroups were included but none of the analyzed xenografts exhibited the profile of ATRT-TYR. The study of Torchia *et al*.[7] classified eight ATRT cell lines as three representing Group 1 (equivalent to ATRT-SHH) and five representing Group 2 (equivalent to ATRT-TYR/ATRT-MYC). However, so far it remained unclear how many of the Group 2 cell lines represent ATRT-TYR (Group 2A) tumors and how many of these represent ATRT-MYC (Group 2B). Aiming to answer this question, we have analyzed the available transcriptomic data for these cell lines. For CHLA02, CHLA04 and CHLA05 the allocation to the ATRT-SHH subgroup is confirmed as expected by unsupervised hierarchical clustering and visualized in the MDS plot (Suppl. Fig. 6). For the remaining cell lines (BT12, BT16, SH, CHLA266, CHLA06), allocation to either ATRT-TYR or ATRT-MYC has so far not been performed. Projection from the MDS plot, correlation analysis and unsupervised clustering (Supplementary Fig. 6A-C) indicate that BT12, BT16, CHLA06, CHL266, and SH, can clearly be allocated to ATRT-MYC. These five cell lines, previously characterized as Group 2, all exhibited high expression of MYC and elevated HOX gene expression in some, but all lacked the TYR group signature (see Suppl. Fig. 6D). Taken together, these data suggests these cell lines are likely all derived from ATRT-MYC tumors.

Additional models have been employed in several other publications investigating drug targets in ATRT xenografts, but the subgroup identity of these models remain unknown. In the cell line BT37 for instance, the role of HMGA2 as an oncogene has been highlighted[21]. This protein is overexpressed specifically in ATRT-TYR (Supplementary Fig. 4), suggesting that BT37 may represent an ATRT-TYR model. While numerous studies have examined drug targets in ATRT irrespective of their subgroup, knowledge on subgroup specific vulnerabilities is sparse. PDGFRB for example, has been shown to be a drug target in Group 2 cell lines BT12, BT16, CHLA266, CHLA06, and SH, and they all displayed a higher susceptibility to PDGFRB inhibitors Nilotinib and Dasatinib than Group 1 (ATRT-SHH) cell lines. Again, whether this means that both ATRT-TYR and ATRT-MYC tumors can be targeted by these inhibitors remains to be seen as PDGFRB expression levels in ATRT-TYR tumors are much higher than in ATRT-MYC tumors (Supplementary Fig. 4). Transcriptome analyses further suggest other promising drug targets that have or have not been tested already in rhabdoid tumors. For instance, *FGFR2* is specifically upregulated in ATRT-TYR and FGFR signaling (together with PDGFR inhibition) has been described as a vulnerability in rhabdoid tumors[22,23]. Another possible candidate is *JAK1*, a protein tyrosine kinase overexpressed in ATRT-TYR that regulates the JAK-STAT signaling cascade. Approved inhibitors such as Ruxolitinib are available and hold the promise of a possible targeted therapy. Further drug screening using robustly subgrouped cell lines will be important to determine which of the prior preclinically tested substances have subgroup specificity.

ATRT-SHH

The ATRT-SHH subgroup, in the Torchia *et al*. publication also referred to as Group 1[7], displays an overexpression of both SHH and NOTCH pathway members, such as for instance *GLI2*, *PTCH1*, and *BOC* (all SHH pathway) or *ASCL1, HES1*, *DTX1* (all regulators of the NOTCH pathway; Supplementary

Fig. 4A). Protein expression of ASCL1, a neuronal differentiation transcription factor, has been suggested as an immunohistochemical marker for this subgroup[6]. Moreover, Torchia *et al*. (2015) showed that ASCL1 protein expression could be a biomarker for improved survival suggesting that ASCL1-positive ATRT-SHH (Group 1) cases have a better overall survival than ASCL1-negative (Group 2) ATRTs[6]. However, as ASCL1 is not expressed in all samples of the SHH subgroup and can also be expressed in some cases of the other subgroups, it remains to be seen whether patients with ATRT-SHH tumors have a better outcome than other ATRT patients. More analyses on prospective cohorts of ATRT patients are needed to see whether there are survival differences between the three molecular subgroups defined by DNA methylation.

Beyond the oncogenic signaling pathways, gene set enrichment analyses confirmed previous observations that ATRT-SHH is mainly a neuronally differentiated subgroup with enrichment of genes involved in “axon guidance pathways” and “neuronal system” pathways, as compared to other subgroups (Fig. 3B).

Torchia *et al*. showed using siRNA and Gamma secretase inhibitors that the Group 1/SHH cell lines dependent on NOTCH signaling for growth[7]. However, therapeutic significance of SHH signaling for ATRT-SHH remains to be tested as unlike SHH-activated medulloblastomas in the MB-SHH subgroup, genomic aberrations of SHH pathway members including *PTCH1, SMO* or *SUFU*, have to date not been found in any ATRT-SHH. All SHH pathway marker genes overexpressed in this subgroup (such as e.g. *GLI2*) are thus most likely directly or indirectly activated by the SMARCB1 loss in these tumors as reported previously[24]. Why SMARCB1 loss does not activate the SHH pathway to the same extent in the other subgroups remains unknown but maybe related to different cellular origin for these subgroups. Thus, whereas clear therapeutic indication for SHH pathway inhibitors has been established for SHH MB, the role of Vismodegib and other SMO inhibitors in ATRTs is unclear and remains to be further investigated[25].

Genetically, ATRT-SHH cases differ from the other two subgroups regarding the type of SMARCB1 alterations. Most ATRT-SHH cases display compound heterozygous point mutations ($p < 0.00025$, chi-square test) as compared to the other groups (Fig. 4C), while homo- or heterozygous *SMARCB1* deletions are less frequently found in this subgroup compared to the other groups (66 from 134 samples, 44% in ATRT-SHH vs 77% in ATRT-TYR and 64% in ATRT-MYC) (Fig. 4D). With regards to age, ATRT-SHH represent a more intermediate subgroup (median age 20 months, range 0 – 96), with patients on average younger than ATRT-MYC patients and older than ATRT-TYR patients.

ATRT-SHH tumors can have either a supratentorial (56/68, 75%) or infratentorial localization (30/68, 35%) (Fig. 4B). However, as reported previously[8], DNA methylation analyses suggest a further molecular heterogeneity within the ATRT-SHH subgroup. Indeed, when performing cluster analyses for ATRT-SHH profiles only, we find that the ATRT-SHH subgroup splits up in two subtypes associated with either a mainly supratentorial location (ATRT-SHH-1) or mainly infratentorial location (ATRT-SHH-2) (Supplementary Fig. 7A-B). The split in two subtypes is supported by consensus clustering when analyzing the SHH subgroup separately (data not shown). It is important to note that both subtypes of ATRT-SHH express marker genes from the NOTCH and SHH pathways. More samples and analyses are needed to investigate whether there are other molecular or clinical differences between these two SHH subtypes. From a radiological point of view, MRI analysis of ATRT-SHH tumors revealed that this is the only subgroup containing tumors that extend both infra- and supratentorially. Moreover, there was a lower degree of contrast enhancement in these tumors compared to ATRT-TYR and ATRT-MYC[19].

With respect to *in vivo* models, the xenograft lines ATRT-310FH and ATRT-311FH have been classified as ATRT-SHH and may thus represent a good tool for future studies[20]. Interestingly, a Rosa26Cre^{ERT2};Smarcb1$^{flox/flox}$ mouse model of rhabdoid tumors reported by Han *et al*. develop spontaneous brain tumors, a subset of which have gene expression profiles very similar to that of human ATRT-SHH (shown in Supplementary Fig. 6A-C)[12]. Similarly, a Snf5 Flox/Flox /p53 lox/lox

/GFAP-Cre (as derived from the study of Ng *et al.*[13]) rhabdoid model seem to be closer to SHH than to the other subgroups. In general development of ATRT in murine models seem to require inactivation of Smarcb1 during early embryonic (E6-E7) development suggesting very early progenitors as cells of origin. Regarding *in vitro* models the CHLA02, CHLA04, and CHLA05 cell lines, all represent ATRT-SHH (formerly Group 1)[7]. Overexpressed drug targets that merit further investigation include the tyrosine kinase DDR1, but also EZH2, which is a candidate drug target for ATRT in general[26]. *In vitro* studies have shown that cell lines derived from ATRT-SHH (Group 1) tumors are more sensitive to EZH2 inhibitors[7]. Of note, recent epigenomic characterizations of primary ATRT suggest EZH2 overexpression in ATRT is not accompanied by global increase of repressive mark H3K27me3[27], indicating additional non-enzymatic functions of EZH2 may be important in ATRTs [28]. Although promising preclinical data have fueled phase I trials using EZH2 inhibitors (e.g. with Tazemetostat, NCT02601937), it remains to be seen if this therapeutic regimen will be efficacious in the clinical setting.

ATRT-MYC

The ATRT-MYC subgroup was named based on elevated expression of the *MYC* oncogene as opposed to the MYCN oncogene which is enriched in the ATRT-SHH group. However, different from other MYC or MYCN-driven pediatric brain tumors like MB-Group 3, MB-SHH, or HGG-MYCN, *MYC or MYCN* amplifications have not been observed respectively in ATRT-MYC or ATRT-SHH tumors. In addition, one of the most striking patterns at the mRNA expression pattern in these tumors is the overexpression of several *HOXC* cluster genes (Fig. 3B), driven by super enhancers[8], i.e. very long stretched enhancers with abundant H3K27ac signal. Similar to ATRT-TYR, a broad categorization into neuronal and mesenchymal subgroups would assign these tumors a more mesenchymal expression profile[7]. The typical genetic pattern that leads to *SMARCB1* inactivation in these tumors is a homozygous, broad loss of *SMARCB1* (which is present in 42/74 cases, 57%), covering several 100

kb[7,8]. In contrast to ATRT-TYR or ATRT-SHH tumors, point mutations are rare in ATRT-MYC tumors (Fig. 4C).

The median age of ATRT-MYC patients is significantly higher than in the two other subgroups (27 months, range 0 - 190.9, Fig. 4A). This is mainly due to a number of older patients and not primarily due to a lack of very young patients in this subgroup.

Although a majority of ATRT-MYC tumors arise supratentorially (25/50, 50%), all spinal tumors in our cohort (6/50, 12%) were of the ATRT-MYC sub-group (Fig. 4B). MRI studies suggest ATRT-MYC tumors are distinguished by presence of a strong peritumoral edema[19]. Of note, recent reports have highlighted similarities between extracranial MRT and ATRT-MYC on the DNA methylation level[29,30]. As the DNA methylation profile of tumor entities is highly reflective of the cell of origin, it raises the question if these entities may share common cellular origins, and whether the behavior of ATRT-MYC tumors may more closely resemble extracranial RTs. Of note, recent studies of adult ATRT suggest these fall mostly in the ATRT-MYC group and suggest further clinical and molecular heterogeneity in ATRT-MYC may be revealed[28].

We have shown here that several cell lines (BT12, BT16, CHLA266, CHLA06, SH) described by Torchia *et al.*[7] (Supplementary Fig. 6C-D) exhibit features more similar to the ATRT-MYC than to the ATRT-TYR subgroup. Several xenograft models of these cell lines suitable for *in vivo* drug testing have been reported[20,31]. Our correlative analysis of GEMM and ATRT primary samples also revealed that as subset of the published tumor samples generated from P0-CreC;Smarcb1 flox/flox mice display high correlation with ATRT-MYC samples and may thus represent a model for the ATRT-MYC subgroup (Suppl. Fig. 6A-B)[14].

Given the previously mentioned similarities between ATRT-MYC and a subgroup of Rhabdoid Kidney tumors (RTK), common molecular targets between extracranial rhabdoid tumors and

subgroups may exist. In fact, Oberlick *et al.*[32] found indeed a dependency of both eMRT and ATRT cell lines on a number of RTKs thus highlighting novel drug targets in these tumors.

Discussion

Identification of distinct molecular subgroups in an otherwise relatively genetically homogeneous disease has been a major step in further understanding the molecular heterogeneity of ATRTs (Fig. 5)[6-8,12]. In this study we aimed to establish a consensus regarding the number of ATRT subgroups, their main molecular and clinical characteristics and a commonly accepted nomenclature in order to enable a better understanding of the clinical heterogeneity in ATRTs. Here, we have shown that the three molecular subgroups identified in previous studies based on DNA methylation and/or gene expression profiling closely match with each other and a consensus was reached to name them ATRT-TYR, ATRT-SHH, and ATRT-MYC, according to the nomenclature published by Johann *et al*.[8] The activated genes or pathways, which were chosen for this nomenclature, emerged when performing overexpression analyses. However, their biological and therapeutic role in ATRT requires further investigation.

A consensus on number and naming of molecular subgroups has in other entities like medulloblastoma[33], ependymoma[34], or glioblastoma[35], proven to be essential for a uniform classification of patient's tumor samples, subgroup specific experiments using properly classified preclinical *in vitro* and *in vivo* models, and ultimately for the design of clinical trials and patient stratification. A further heterogeneity within these main three ATRT subgroups may still exist, similar to what has been reported for medulloblastoma or ependymoma subgroups for instance[36,37]. Thus far, DNA methylation profiling has identified two further subtypes within the ATRT-SHH subgroup, which correlates with predominant supratentorial (ATRT-SHH-1) or infratentorial locations (ATRT-

SHH-2), but larger cohort studies are needed to better define molecular differences between these subtypes and whether they are clinically relevant.

As the outcome for ATRT patients is still relatively poor, new treatment strategies are urgently needed. Identification and characterization of ATRT subgroups may help discovery of subgroup specific treatments, but will also help to elucidate new pan-ATRT therapies. Given the reported relatedness of ATRT-MYC to extracranial rhabdoids, these investigations should also include extracranial malignant rhabdoid tumors (MRT) such as those occurring in the kidney, liver, or other soft tissues[29,38]. Additionally, more molecularly characterized models, including cell lines, patient-derived orthotopic xenograft models and tumor organoid cultures, which represent the molecular spectrum of ATRTs are needed to critically advance ATRT therapeutics.

The prognostic value of the ATRT subgroups remains to be fully investigated. Torchia *et al.* reported ASCL1 protein expression, which is highly expressed in ATRT-SHH, was associated with a better outcome[6]. However, it is not clear whether this is true for the whole SHH subgroup as not all ATRT-SHH cases may express ASCL1. There clearly is a need for assessing the predictive power of the subgroups in well characterized cohorts in prospective, clinical studies.

Finally, to get a better understanding of the clinical relevance of ATRTs subgroups, molecular subgrouping should be included in any future clinical trial for ATRT patients. The method of choice is currently DNA methylation profiling as this requires very little input material (tumor DNA isolated from either frozen or formalin-fixed paraffin-embedded tumor tissue), and shows little or no bias when performed at different centers. However, as DNA methylation profiling may not always be available, it would still be helpful if more readily available markers or methods to subgroup ATRTs, such as immunohistochemical staining for tyrosinase or ASCL1, or Nanostring subgrouping methods as has been developed for medulloblastoma, could also be developed for broader use in clinical labs globally.

Acknowledgements

The authors would like to thank their national and international colleagues for providing ATRT samples and associated clinical data for this study.

References

1. Fruhwald MC, Biegel JA, Bourdeaut F, Roberts CW, Chi SN. Atypical teratoid/rhabdoid tumors-current concepts, advances in biology, and potential future therapies. *Neuro Oncol.* 2016; 18(6):764-778.
2. Hasselblatt M, Nagel I, Oyen F, et al. SMARCA4-mutated atypical teratoid/rhabdoid tumors are associated with inherited germline alterations and poor prognosis. *Acta Neuropathologica.* 2014; 128(3):453-456.
3. Schneppenheim R, Fruhwald MC, Gesk S, et al. Germline nonsense mutation and somatic inactivation of SMARCA4/BRG1 in a family with rhabdoid tumor predisposition syndrome. *Am J Human Gen.* 2010; 86(2):279-284.
4. Ginn KF, Gajjar A. Atypical teratoid rhabdoid tumor: current therapy and future directions. *Front Oncol.* 2012; 2:114.
5. Birks DK, Donson AM, Patel PR, et al. High expression of BMP pathway genes distinguishes a subset of atypical teratoid/rhabdoid tumors associated with shorter survival. *Neuro Oncol.* 2011; 13(12):1296-1307.
6. Torchia J, Picard D, Lafay-Cousin L, et al. Molecular subgroups of atypical teratoid rhabdoid tumours in children: an integrated genomic and clinicopathological analysis. *Lancet Oncol.* 2015; 16(5):569-582.
7. Torchia J, Golbourn B, Feng S, et al. Integrated (epi)-Genomic Analyses Identify Subgroup-Specific Therapeutic Targets in CNS Rhabdoid Tumors. *Cancer Cell.* 2016; 30(6):891-908.
8. Johann PD, Erkek S, Zapatka M, et al. Atypical Teratoid/Rhabdoid Tumors Are Comprised of Three Epigenetic Subgroups with Distinct Enhancer Landscapes. *Cancer Cell.* 2016; 29(3):379-393.
9. Capper D, Jones DTW, Sill M, et al. DNA methylation-based classification of central nervous system tumours. *Nature.* 2018; 555(7697):469-474.
10. Schwalbe EC, Lindsey JC, Nakjang S, et al. Novel molecular subgroups for clinical classification and outcome prediction in childhood medulloblastoma: a cohort study. *Lancet Oncol.* 2017; 18(7):958-971.
11. Sharma T, Schwalbe EC, Williamson D, et al. Second-generation molecular subgrouping of medulloblastoma: an international meta-analysis of Group 3 and Group 4 subtypes. *Acta Neuropathol.* 2019; 138(2):309-326.
12. Han ZY, Richer W, Freneaux P, et al. The occurrence of intracranial rhabdoid tumours in mice depends on temporal control of Smarcb1 inactivation. *Nat Commun.* 2016; 7:10421.
13. Ng JM, Martinez D, Marsh ED, et al. Generation of a mouse model of atypical teratoid/rhabdoid tumor of the central nervous system through combined deletion of Snf5 and p53. *Cancer Res.* 2015; 75(21):4629-4639.
14. Vitte J, Gao F, Coppola G, Judkins AR, Giovannini M. Timing of Smarcb1 and Nf2 inactivation determines schwannoma versus rhabdoid tumor development. *Nat Commun.* 2017; 8(1):300.
15. Hasselblatt M, Thomas C, Nemes K, et al. Tyrosinase immunohistochemistry can be employed for the diagnosis of atypical teratoid/rhabdoid tumours of the tyrosinase subgroup (ATRT-TYR). *Neuropathol Appl Neurobiol.* 2019. doi: 10.1111/nan.12560
16. Simoes-Costa M, Bronner ME. Establishing neural crest identity: a gene regulatory recipe. *Development.* 2015; 142(2):242-257.
17. Tief K, Schmidt A, Aguzzi A, Beermann F. Tyrosinase is a new marker for cell populations in the mouse neural tube. *Dev Dyn.* 1996; 205(4):445-456.
18. Johann PD, Hovestadt V, Thomas C, et al. Cribriform neuroepithelial tumor: molecular characterization of a SMARCB1-deficient non-rhabdoid tumor with favorable long-term outcome. *Brain Pathol.* 2017; 27(4):411-418.

19. Nowak J, Nemes K, Hohm A, et al. Magnetic resonance imaging surrogates of molecular subgroups in atypical teratoid / rhabdoid tumor (ATRT). *Neuro Oncol.* 2018.

20. Brabetz S, Leary SES, Grobner SN, et al. A biobank of patient-derived pediatric brain tumor models. *Nat Med.* 2018; 24(11):1752-1761.

21. Kaur H, Hutt-Cabezas M, Weingart MF, et al. The chromatin-modifying protein HMGA2 promotes atypical teratoid/rhabdoid cell tumorigenicity. *J Neuropathol Exp Neurol.* 2015; 74(2):177-185.

22. Wong JP, Todd JR, Finetti MA, et al. Dual Targeting of PDGFRalpha and FGFR1 Displays Synergistic Efficacy in Malignant Rhabdoid Tumors. *Cell Rep.* 2016; 17(5):1265-1275.

23. Chauvin C, Leruste A, Tauziede-Espariat A, et al. High-Throughput Drug Screening Identifies Pazopanib and Clofilium Tosylate as Promising Treatments for Malignant Rhabdoid Tumors. *Cell Rep.* 2017; 21(7):1737-1745.

24. Jagani Z, Mora-Blanco EL, Sansam CG, et al. Loss of the tumor suppressor Snf5 leads to aberrant activation of the Hedgehog-Gli pathway. *Nat Med.* 2010; 16(12):1429-1433.

25. Kerl K, Moreno N, Holsten T, et al. Arsenic trioxide inhibits tumor cell growth in malignant rhabdoid tumors in vitro and in vivo by targeting overexpressed Gli1. *Int J Cancer.* 2014; 135(4):989-995.

26. Knutson SK, Kawano S, Minoshima Y, et al. Selective inhibition of EZH2 by EPZ-6438 leads to potent antitumor activity in EZH2-mutant non-Hodgkin lymphoma. *Mol Cancer Ther.* 2014; 13(4):842-854.

27. Erkek S, Johann PD, Finetti MA, et al. Comprehensive Analysis of Chromatin States in Atypical Teratoid/Rhabdoid Tumor Identifies Diverging Roles for SWI/SNF and Polycomb in Gene Regulation. *Cancer Cell.* 2019; 35(1):95-110 e118.

28. Alig SK, Dreyling M, Seppi B, Aulinger B, Witkowski L, Rieger CT. Severe cytokine release syndrome after the first dose of Brentuximab Vedotin in a patient with relapsed systemic anaplastic large cell lymphoma (sALCL): a case report and review of literature. *Eur J Haematol.* 2015; 94(6):554-557.

29. Pinto EM, Hamideh D, Bahrami A, et al. Malignant rhabdoid tumors originating within and outside the central nervous system are clinically and molecularly heterogeneous. *Acta Neuropathologica.* 2018; 136(2):315-326.

30. Chun HE, Johann PD, Milne K, et al. Identification and Analyses of Extra-Cranial and Cranial Rhabdoid Tumor Molecular Subgroups Reveal Tumors with Cytotoxic T Cell Infiltration. *Cell Rep.* 2019; 29(8):2338-2354 e2337.

31. Hashizume R, Zhang A, Mueller S, et al. Inhibition of DNA damage repair by the CDK4/6 inhibitor palbociclib delays irradiated intracranial atypical teratoid rhabdoid tumor and glioblastoma xenograft regrowth. *Neuro Oncol.* 2016; 18(11):1519-1528.

32. Oberlick EM, Rees MG, Seashore-Ludlow B, et al. Small-Molecule and CRISPR Screening Converge to Reveal Receptor Tyrosine Kinase Dependencies in Pediatric Rhabdoid Tumors. *Cell Rep.* 2019; 28(9):2331-2344 e2338.

33. Taylor MD, Northcott PA, Korshunov A, et al. Molecular subgroups of medulloblastoma: the current consensus. *Acta Neuropathologica.* 2012; 123(4):465-472.

34. Pajtler KW, Mack SC, Ramaswamy V, et al. The current consensus on the clinical management of intracranial ependymoma and its distinct molecular variants. *Acta Neuropathologica.* 2017; 133(1):5-12.

35. Sturm D, Witt H, Hovestadt V, et al. Hotspot mutations in H3F3A and IDH1 define distinct epigenetic and biological subgroups of glioblastoma. *Cancer Cell.* 2012; 22(4):425-437.

36. Cavalli FMG, Hubner JM, Sharma T, et al. Heterogeneity within the PF-EPN-B ependymoma subgroup. *Acta Neuropathologica.* 2018; 136(2):227-237.

37. Cavalli FMG, Remke M, Rampasek L, et al. Intertumoral Heterogeneity within Medulloblastoma Subgroups. *Cancer Cell.* 2017; 31(6):737-754 e736.

38. Chun HE, Johann PD, Milne K, et al. Identification and Analyses of Extra-Cranial and Cranial Rhabdoid Tumor Molecular Subgroups Reveal Tumors with Cytotoxic T Cell Infiltration. *Cell Rep.* 2019.

Figure legends:

Figure 1: **Overview flow charts on all analyses and samples.**

Figure 2: **Methylation array analysis of the consensus dataset.**

a) Unsupervised hierarchical Clustering using the top 5000 most variable CG sites confirms the presence of three subgroups in the consensus dataset (325 samples).

b) *t*-SNE visualization of the analyzed dataset based on the 5000 most variable CG sites reproduces segregation into three main ATRT subgroups. Coloring of data points in the *t*-SNE plots displays the subgrouping as published in Johann *et al.*[8] (upper plot) or in Torchia *et al.*[7] (lower plot). Half transparent circles show the consensus subgroups used in this paper.

c) Sankey plot displaying the concordance between the subgroup calls using different methods (NMF, Consensus Clustering and NMF+KM based subgrouping). Numbers in each subgroup show the number of samples which have been assigned to the subgroup with the respective method.

Figure 3: Cluster analysis based on Affymetrix array gene expression data.

a) Unsupervised hierarchical clustering using the top 1500 most variable genes in the consensus gene expression dataset. Annotations in the lower bar show the grouping as presented in Han *et al*.[12] and in Johann *et al*.[8] and the current methylation consensus calls.

b) Visualization of GSEA results as a radar plot. Axis displays the normalized enrichment values. Each ATRT subgroup is represented in the respective subgroup color.

Figure 4: **Clinical and genetic associations of ATRT subgroups.**

a) Violin plots of age distribution in ATRT subgroups.

b) Frequency of CNS tumor location by consensus subgroup represented by pie charts.

c) Oncoprint figure displays the distribution of various types of SMARCB1 mutations among the consensus set.

d) Distribution of SMARCB1 alterations and chr22 changes in the consensus set as determined by methylation array analyses, represented by pie charts.

Significance between subgroups was calculated with chi square test.

Figure 5: Consensus overview on ATRT subgroups.

Schema of salient clinical and molecular characteristics of ATRT subgroups.

Study	Subgroups			Methods/platforms used (n = # cases)
Torchia *et al*., 2015	**Group 1** Overexpression of ASCL1	**Group 2**		**Immunohistochemistry** (ASCL1) (n = 170) **Gene expression array profiling** (Illumina HT12) (n = 43)
Torchia *et al*., 2016	**Group 1** Overexpression of NOTCH pathway genes ASCL1, CBL, HES1	**Group 2A** Overexpression of neuronal and mesenchymal genes OTX2, PDGFRB, BMP4	**Group 2B** Overexpression of HOX cluster genes	**Methylation array profiling** (Illumina 450K) (n = 162) **Gene expression array profiling** (Illumina HT12) (n = 90)
Johann *et al*., 2016	**ATRT-SHH** Overexpression of SHH pathway genes GLI2, BOC, PTCHD2, MYCN	**ATRT-TYR** Overexpression of melanosomal genes TYR, TYRP, MITF, OTX2	**ATRT-MYC** Overexpression of MYC and HOX cluster genes	**Methylation array profiling** (Illumina 450K) (n = 150) **Gene expression array profiling** (Affymetrix U133plus2.0) (n = 69)
Han *et al*., 2016	**hIC2** Overexpression of ASCL1, BOC, SOX2, GLI2, FABP7	**hIC1** Overexpression of BMP4, OTX2, SMAD7	**hIC3** Overexpression of ACTL6A, FABP7, GFAP	**Gene expression array profiling** (Affymetrix U133plus2.0) (n = 30)

Table 1: Summary of defining transcriptional features of ATRT subgroups. Data derived from publications [8-10].

Figure 1

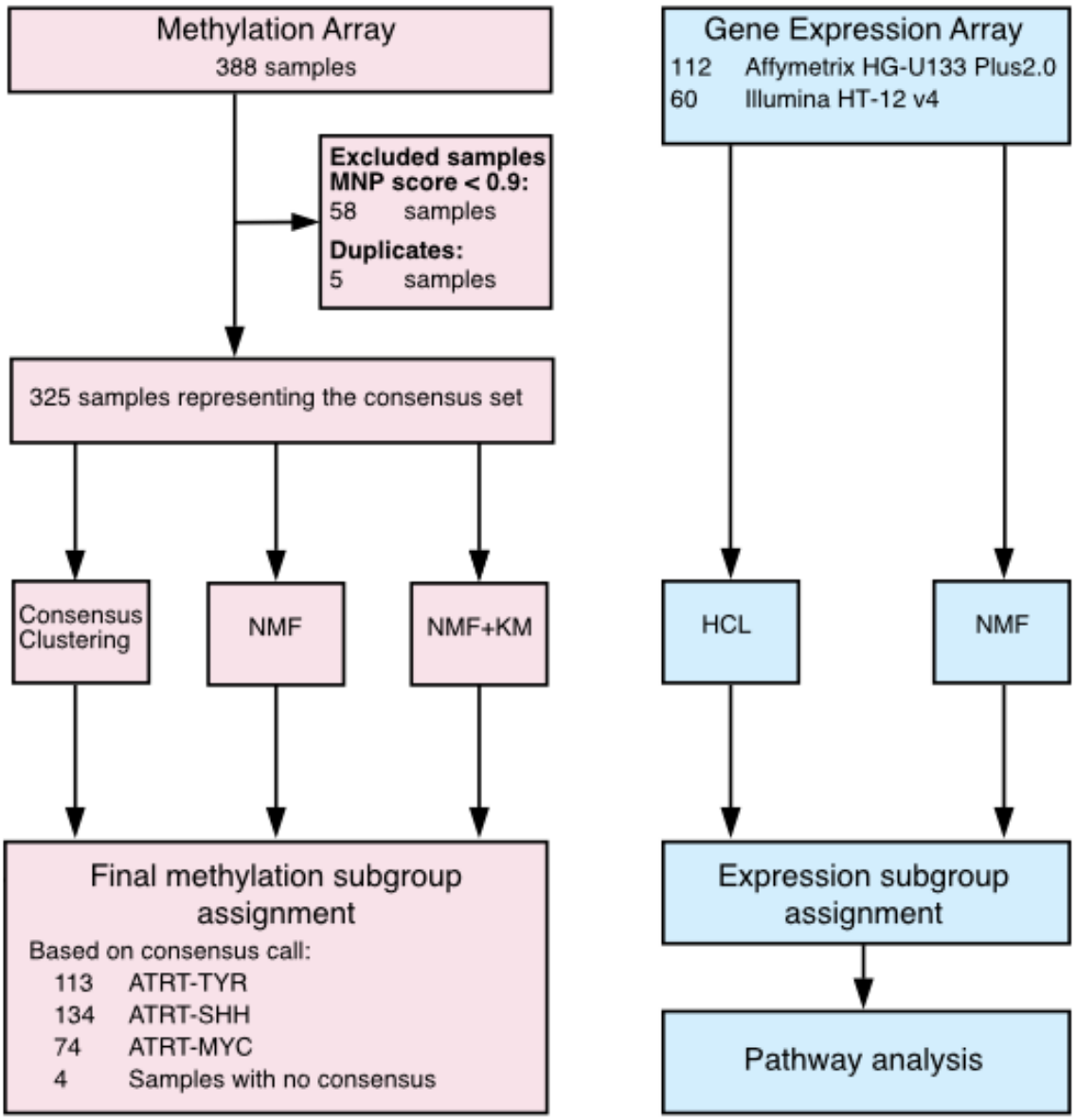

Figure 2

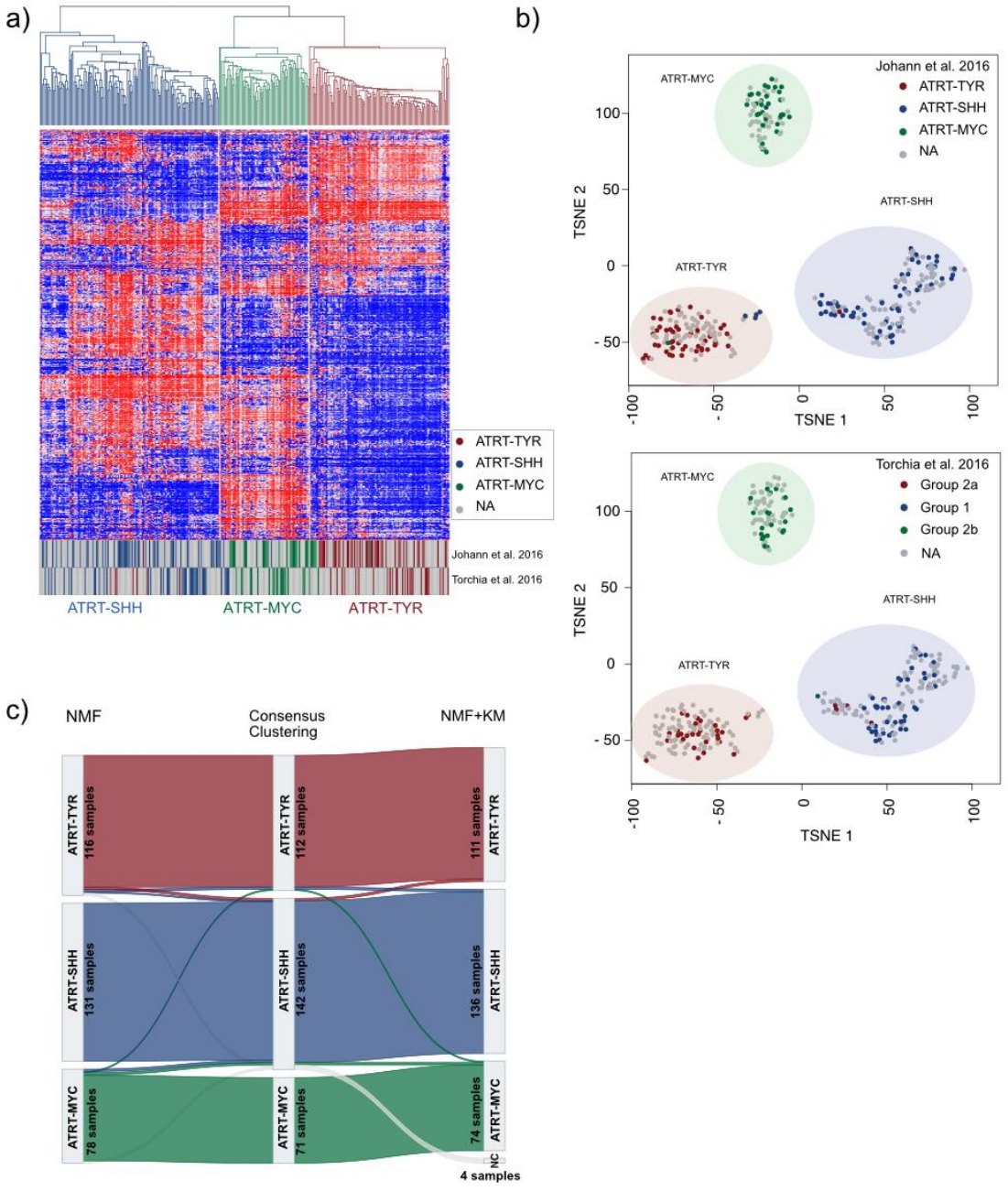

Figure 3

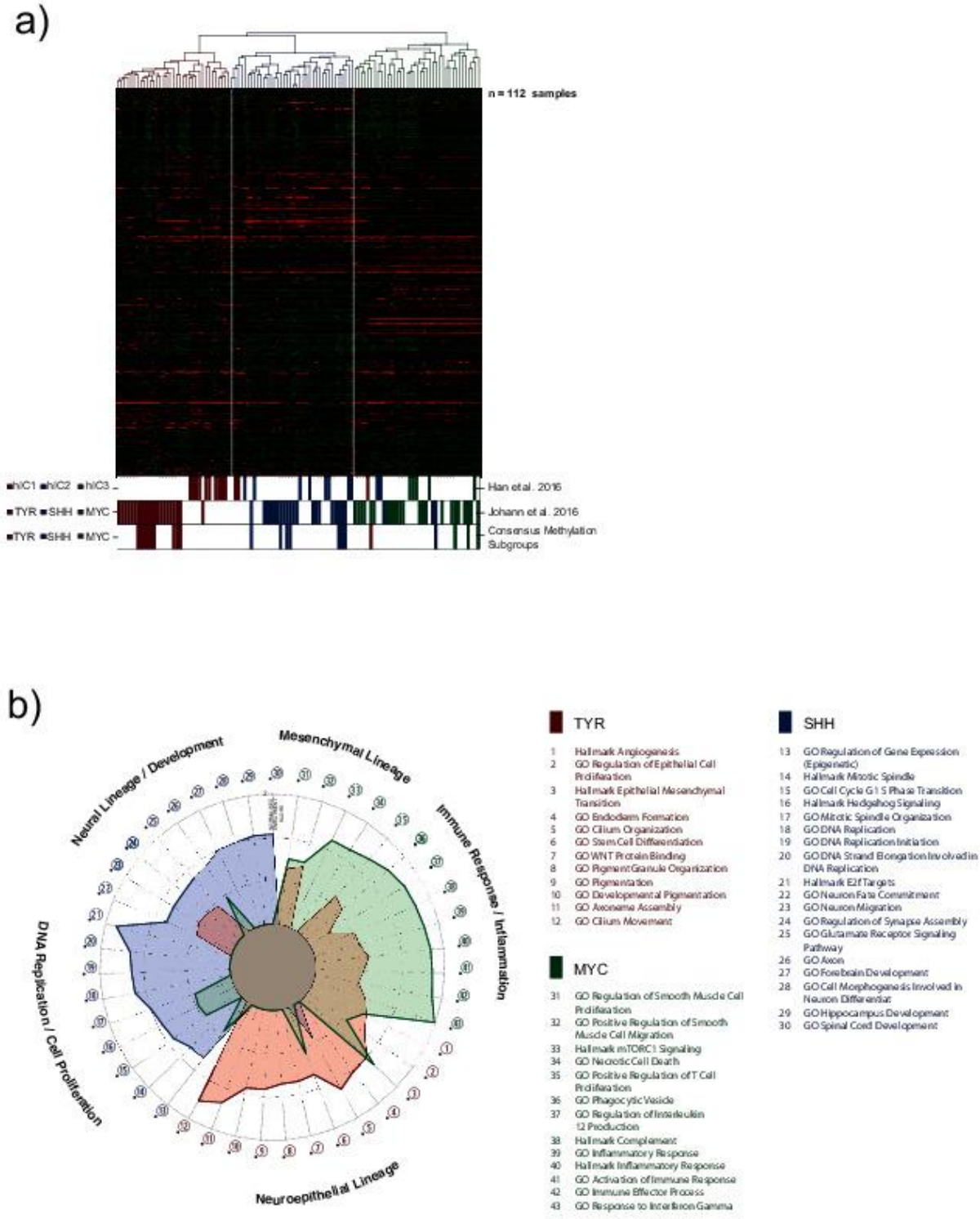

Figure 4

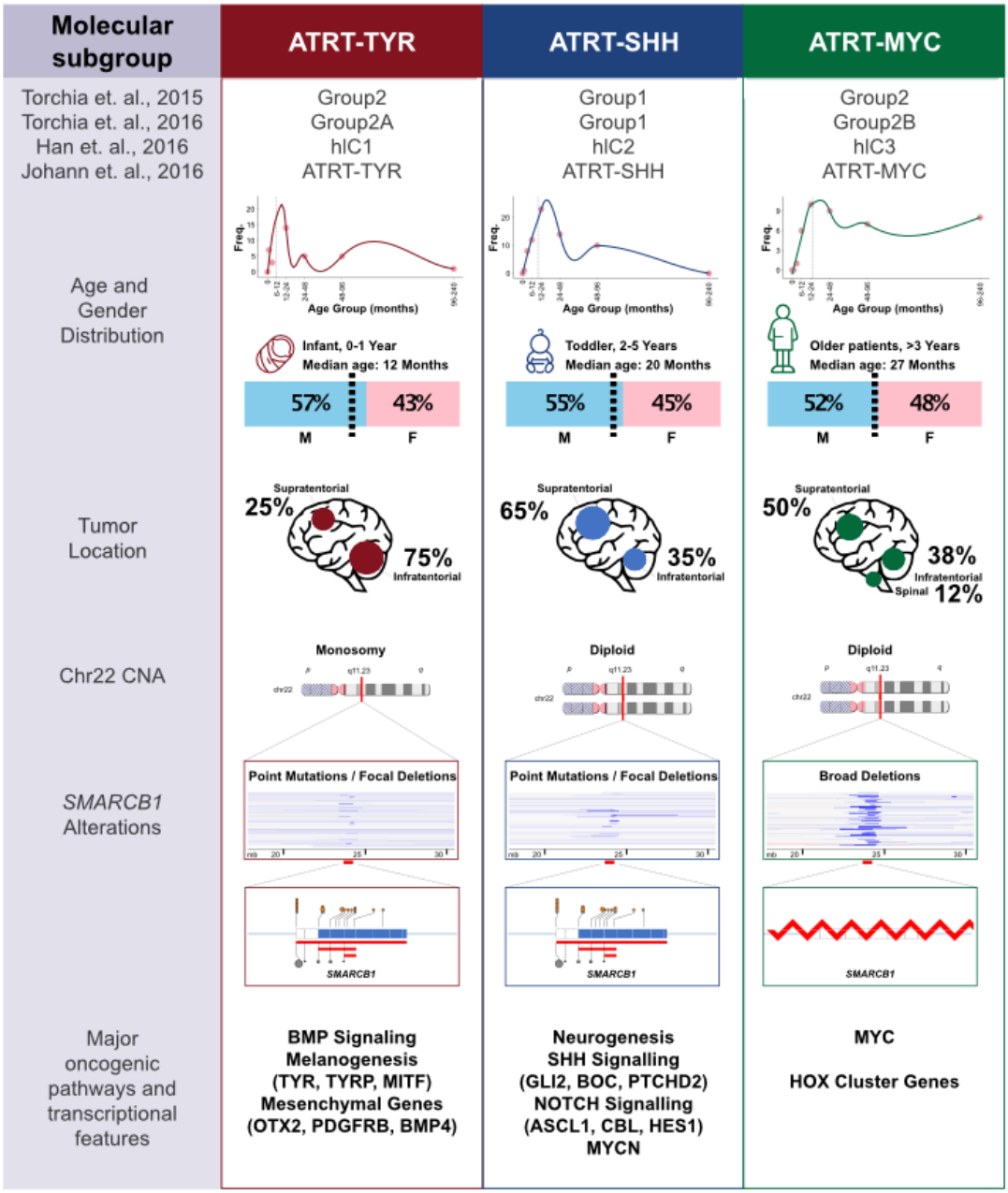

Figure 5